Utrecht University

Developing a tool to temporally degrade proteins

By

Rik Bouwels (8260737)

A Master's Thesis

Submitted to the Chaigne Lab

Department of Cell Biology, Neurobiology and Biophysics

Utrecht University

Supervised by

Snježana Kodba (PhD Candidate)

Amber Öztop (PhD Candidate)

Agathe Chaigne (Asst. Prof.)

Graphical Abstract

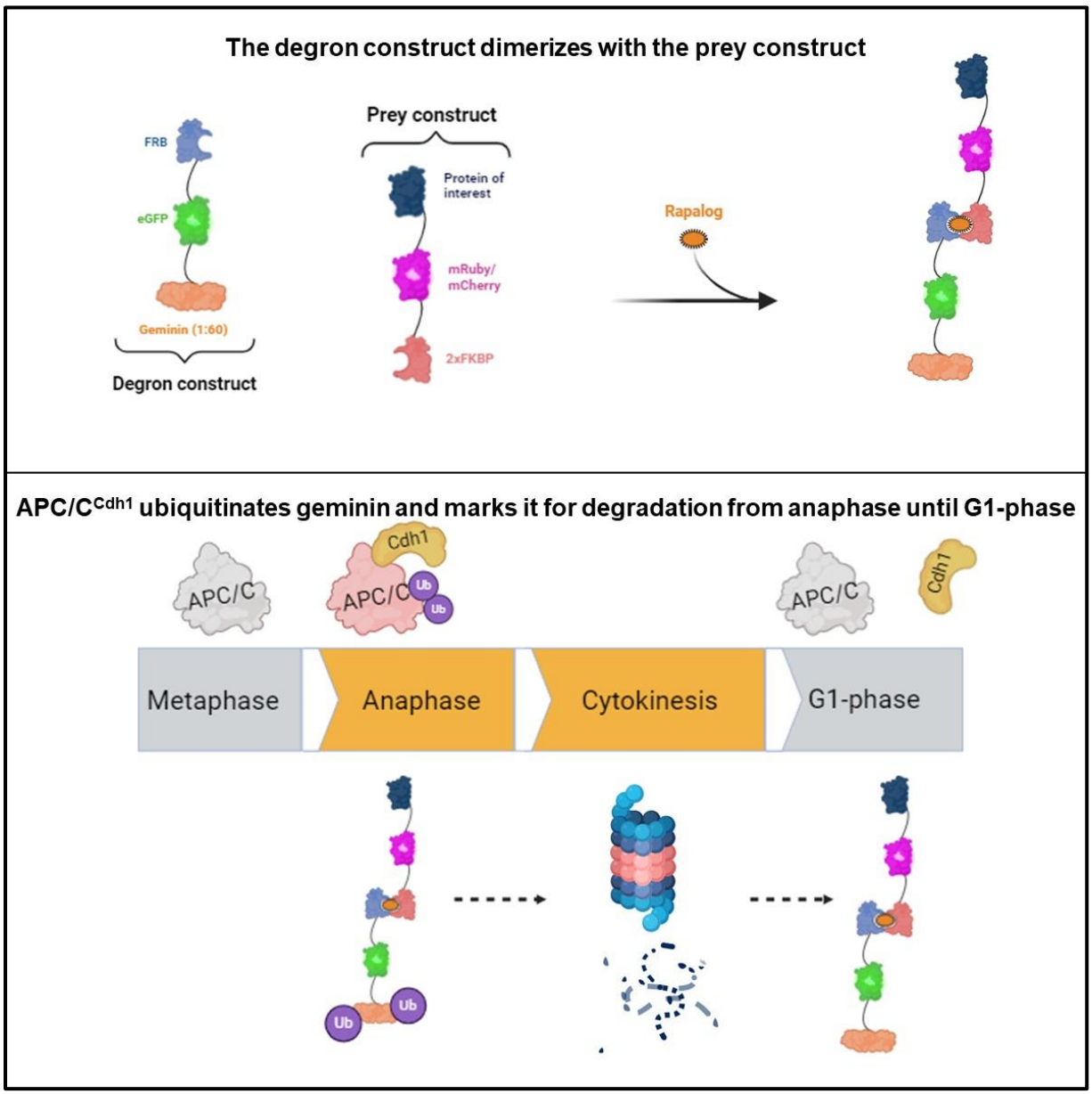

Table of Contents

Lay summary

One mother cell divides into two daughter cells, a process that is necessary for life. This process involves many steps to make sure that the genetic material is accurately copied and passed on to the two daughter cells. For these steps to work in the right order, certain proteins must be broken down at the right moments. The cell has a built-in system to target proteins and break them down when they are no longer necessary. One mechanism by which the cell achieves this is by connecting a very specific destruction signal to these proteins. Proteins that are connected to a destruction signal are then picked up by a large destruction machine that breaks them down into their basic building blocks.

Researchers have developed methods to block and break down proteins themselves to study their function in the division process of cells. However, each method comes with its strengths and limitations. For example, researchers use certain drugs to block a protein they want to study, by which it can no longer carry out its function but this might affect unintended proteins as well. Researchers can also remove the genetic material that forms a protein, blocking its production. This method is very specific but results in the permanent removal of proteins with drastic consequences for the cell division process.

To overcome these limitations, we are developing a method to break down specific proteins only during the latest stages of cell division. Our method is based on a two-part system. Firstly, we attach a destruction signal to the proteins we want to study. This destruction signal is part of a protein called geminin. This is important because geminin is only broken down during the final stages of cell division. For ease, we will call this destruction signal the degron. Secondly, we attach a binding domain to our protein of interest, which we will call the ‘’prey’’ because our degron targets it. This binding domain makes sure that the prey will connect to the degron after we add a specific drug. To activate the system, we add the drug, which acts like a remote control for our system. As a consequence, it triggers the cell to start breaking down the connected proteins only during the final stages of cell division. We can then use advanced imaging techniques to observe and track this process in real time, allowing us to see exactly how and when the proteins are broken down.

Our experiments show that the degron alone is broken down only at the final stages of cell division, which is the essence of our degron. We then added the drug to connect it to proteins of interest. However, we observed that this connection does often not take place and more importantly, that our protein of interest is not broken down after it forms a connection to our degron. Therefore, we need to carry out troubleshooting experiments to improve the low efficiency of our connection and to find out why our protein of interest does not break down at the final stage of cell division.

In summary, our research forms the foundation for a method to control specific protein breakdown only at the final stage of cell division. However, challenges must be overcome to make this method work effectively.

Abstract

To investigate the effects of proteins on cellular processes, researchers employ a variety of strategies to modulate protein expression levels. Current methods include genomic approaches like CRISPR-Cas9 knockouts, post-transcriptional approaches such as RNA interference, and protein-level approaches using chemical inhibitors and inducible degron systems. However, these strategies cannot control protein expression levels during specific cell cycle stages. To address this limitation, we aimed to develop a novel inducible system for temporal protein degradation from anaphase onset until G_1-phase by using the ubiquitinase activity of the anaphase-promoting complex/cyclosome. Inspired by the fluorescent cell cycle reporter (Fucci) system, we linked geminin (hGem), a direct substrate of APC/C, to proteins of interest. Two constructs were developed: (I) hGem(1:60) linked to eGFP and FRB (the degron), and (II) two FKBP domains linked to mCherry or mRuby and the protein of interest (the prey). Live-cell imaging demonstrated that the degron construct degrades after anaphase onset. Fixed-cell imaging demonstrated recruitment of degron counterparts to prey constructs, while live-cell imaging revealed proteasomal degradation of the degron but not the prey after anaphase onset. Colocalization analysis indicated dimerization in only 20% of cells, by which degron constructs are protected from degradation. We hypothesize that the low efficiency of rapalog-induced dimerization and subsequent protection from degradation are distinct challenges, both of which could be explained by individual steps in the experimental design. This thesis lays the foundation for the temporal perturbation of proteins from anaphase until G_1-phase and identifies challenges for the development of this system.

Introduction

Controlling protein abundance is necessary to study their function in cellular processes. Researchers employed various strategies to limit protein expression levels of which each has its advantages and limitations. At the genomic level, gene editing approaches such as CRISPR-Cas9 knockouts are used to delete genes encoding the protein of interest. While these methods allow precise control over protein expression, they result in the permanent removal of target proteins which can potentially cause off-target effects[1]. At the post-transcriptional level, approaches such as RNA interference and RNA drugs regulate mRNA levels, allowing for precise control and reversibility. However, these methods do not facilitate temporal control of protein abundance during specific cell cycle phases[2]. At the protein level, chemical inhibitors, such as ZM447439 for aurora kinases, can rapidly and reversibly stabilize proteins with little off-target effects[3]. Despite this, some proteins lack specific chemical inhibitors[4,5], by which the approach is limited. Auxin-inducible degron (AID) systems resolve this problem by utilizing the plant hormone auxin to induce the degradation of tagged proteins, but they do not provide temporal control during specific phases of the cell cycle[6].

To overcome the limitation of temporal control, we aim to develop a novel inducible and temporal method to degrade proteins of interest, specifically during cytokinesis. Our strategy is inspired by the Fluorescent Ubiquitination-based Cell Cycle Indicator (Fucci), which uses fluorescent probes to visualize cell cycle phases[7]. The Fucci system takes advantage of the cell cycle-dependent degradation of key regulatory proteins. One such regulatory protein is geminin, which is a direct substrate of the anaphase-promoting complex/cyclosome (APC/C) when activated by Cdh1 (APC/C^{Cdh1})[8]. Upon anaphase onset, APC/C^{Cdh1} activates, which leads to the rapid ubiquitination and subsequent degradation of geminin by the 26S proteasome. Degradation continues until G_1-phase, when Cdh1 dislodges and deactivates the APC/C[9].

Building on this concept, we aim to link geminin to proteins of interest to achieve temporal degradation of these proteins from anaphase until G_1-phase. The degron system involves two parts: the first construct, termed ‘the degron’, comprises the first 60 amino acids of geminin (hGem(1:60)), eGFP, and an FRB domain. The second construct, termed ‘the prey’, consists of two FKBP domains, mCherry or mRuby, and the protein of interest (Figure 1A). The interaction between the FRB and FKBP domain, induced by the drug rapalog[10], allows for reversible[11] dimerization between the degron and prey parts. This strategy employs the cell’s endogenous degradation machinery to degrade proteins, avoiding the need for chemical inhibitors or depletion methods.

In this thesis, we investigate whether APC/C^{Cdh1} can be utilized to develop an inducible system for the temporal degradation of proteins linked to cytokinesis from anaphase until G_1-phase. Using live-cell imaging, we demonstrate that the degron construct degrades after anaphase onset (Figure 1B) and that the degron construct is capable of recruiting prey constructs (Figure 2B). However, live-cell imaging of the degron and various prey constructs revealed different localization patterns leading to differential degradation outcomes (Figure 3). We suspect that the low efficiency of rapalog-induced dimerization and the subsequent protection from degradation are two distinct challenges and discuss various hypotheses for these observations. This thesis lays the foundation for a system to temporally control proteins from anaphase until G_1-phase. It also highlights new challenges that must be overcome before this exogenous system can be adapted to an endogenous system to achieve precise temporal degradation of proteins.

Results

The degron construct degrades after anaphase onset

To validate the functionality of the degron construct, we first aimed to demonstrate that geminin degrades after anaphase onset. Therefore, we used U2OS cells stably expressing the degron construct (hGem(1:60)-eGFP-FRB) upon doxycycline induction. In these experiments, we tracked the fluorescence of eGFP, which is linked to the degron, across multiple time points before and after anaphase onset (Figure 1B). In U2OS$^{hGem(1:60)\text{-}eGFP\text{-}FRB}$ cells, we observed a high degron-eGFP signal before anaphase onset. At anaphase onset (timepoint 0), there is a large decrease in eGFP fluorescence over time, indicating that the degron is being degraded (Figure 1C) These observations confirm that the degron construct is targeted for degradation after anaphase onset.

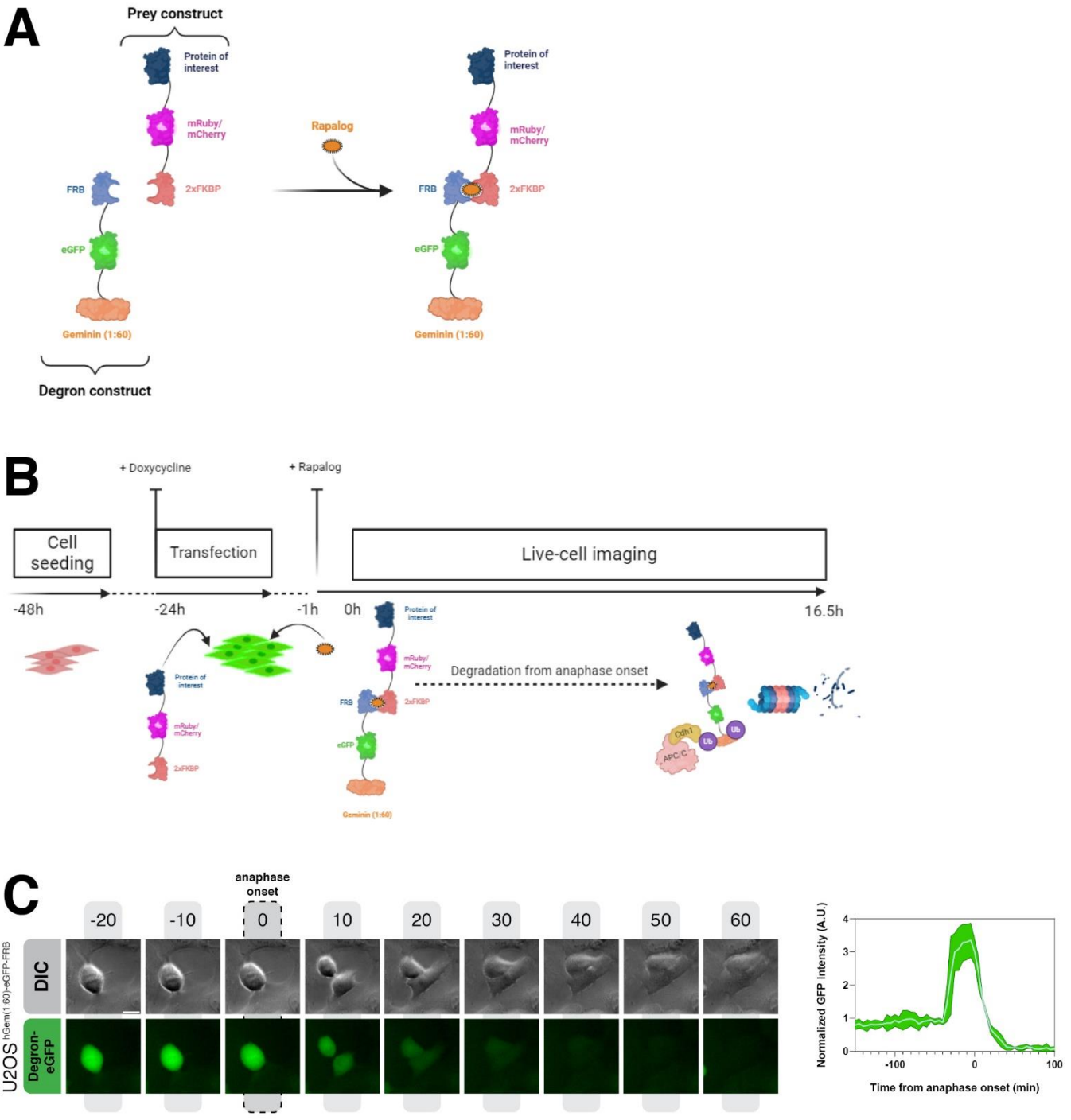

Figure 1. The degron construct degrades after anaphase onset.

(A) Schematic representation of the degron system. The degron construct consists of hGem(1:60) linked to eGFP, and an FRB domain. The prey constructs include various proteins of interest linked with mCherry/mRuby, and two FKBP domains. The presence of rapalog facilitates dimerization between the FRB and FKBP domains, linking the degron and the prey constructs. **(B)** Schematic representation of the experimental workflow for live-cell imaging to study colocalization and degradation. **(C)** Live-cell imaging of U2OS$^{hGem(1:60)\text{-}eGFP\text{-}FRB}$ cells expressing hGem(1:60)-eGFP-FRB upon doxycycline induction. The images show differential interference contrast (DIC) and degron-eGFP expression at various timepoints relative to anaphase onset (time 0). The corresponding graph shows the quantification of the degron-eGFP signal over time. The X-axis indicates the time from anaphase onset, whereas the Y-axis indicates the normalized eGFP expression as a fraction of the average intensity per timepoint (mean ± s.d. of three representative cells across one independent experiment).

The degron construct can recruit prey constructs

Cells can degrade the degron construct after anaphase onset. Next, we investigated whether prey constructs (2xFKBP-mRuby/mCherry-protein of interest) can be recruited to the degron construct by the addition of rapalog. For this purpose, we transfected U2OS cells stably expressing the degron construct and transfected HeLa cells with both the degron and prey constructs (Figure 2A). As prey constructs, we used three different proteins (Vimentin, AKAP1, and Rab11) with distinct localization patterns. Vimentin is a cytoskeletal component that localizes in a filamentous pattern, AKAP1 is a mitochondrial anchoring protein that localizes to mitochondria, and Rab11 is involved in endosomal recycling and localizes to endosomes.

In both U2OS$^{hGem(1:60)\text{-}eGFP\text{-}FRB}$ cells and HeLa cells, the degron-eGFP signal localized cytoplasmic and nuclear the absence of rapalog, showing no colocalization with the prey constructs. However, in the presence of rapalog, the degron-eGFP signal colocalizes with prey-mRuby/mCherry signals. When using the vimentin-prey construct, the degron-eGFP signal displayed a filamentous localization pattern at the cell periphery. With the AKAP1-prey construct, the degron-eGFP signal was observed at mitochondrial structures. Similarly, when using the Rab11-prey construct, the degron-eGFP signal colocalized with endosomes, indicated by the dot structure. These results demonstrate that rapalog effectively induces the recruitment of the degron construct to prey constructs.

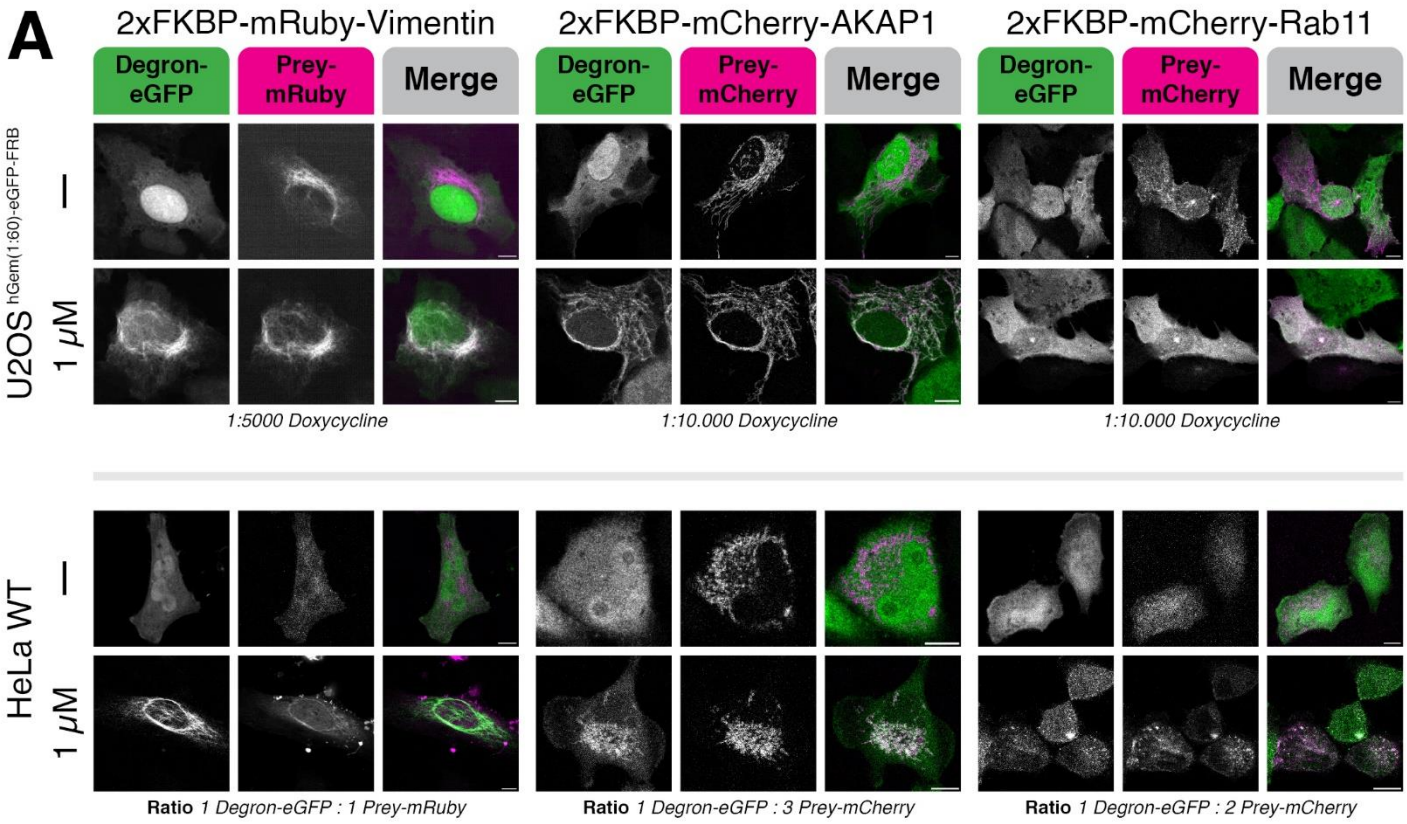

Figure 2. Recruitment of prey constructs to degron constructs in U2OS$^{hGem(1:60)\text{-}eGFP\text{-}FRB}$ cells and HeLa WT cells.

(A) Fixed-cell imaging displaying U2OS$^{hGem(1:60)\text{-}eGFP\text{-}FRB}$ cells (upper panel) and HeLa cells transfected with hGem(1:60)-eGFP-FRB (lower panel). Localization patterns of hGem(1:60)-eGFP-FRB and three different prey constructs (2xFKBP-mRuby-Vimentin (left panel), 2xFKBP-mCherry-AKAP1 (middle panel), and 2xFKBP-mCherry-Rab11 (right panel)). Cells were either left untreated (-) or treated with rapalog. For U2OS$^{hGem(1:60)\text{-}eGFP\text{-}FRB}$ cells, different concentrations of Doxycycline were used for induced-expression as indicated below the panels. For HeLa WT cells, the used ratios between the degron and prey constructs are indicated below the panels. n=3 cells per condition across one independent experiment.

Degradation dynamics of the degron and prey constructs

We demonstrated that the degron construct degrades after anaphase onset and that the degron construct can recruit prey constructs. To investigate the degradation dynamics of the degron construct and various prey constructs in the presence of rapalog, we performed live-cell imaging on U2OS$^{hGem(1:60)\text{-}eGFP\text{-}FRB}$ cells transfected with AKAP1 as prey construct (Figure 3A).

In the absence of rapalog, the degron construct displayed a uniform distribution across the cell, showing no specific colocalization to mitochondria as opposed to the AKAP1-prey construct. Consequently, the degron construct was rapidly degraded after anaphase onset, as indicated by a decreasing degron-eGFP signal in the adjacent graph. The prey-mCherry signal is expectedly maintained after anaphase onset. In the presence of rapalog, we observed a shift in the localization pattern of the degron construct. The degron construct was recruited to the mitochondria, as indicated by overlapping degron-eGFP and prey-mCherry signals. The colocalization partially protected the degron construct from degradation, maintaining the degron-eGFP signal after anaphase onset. The corresponding prey-mCherry graph is highly similar to the degron-eGFP graph, indicating that the AKAP1-prey construct colocalizes with the degron construct. Interestingly, the prey-mCherry signal increased after anaphase onset, indicating that the AKAP1-prey construct is not degraded.

Next, we performed live-cell imaging on U2OS$^{hGem(1:60)\text{-}eGFP\text{-}FRB}$ cells transfected with vimentin as prey construct (Figure 3B). In the absence of rapalog, the degron again displayed a uniform distribution across the cell as opposed to the Vimentin-prey construct. Similarly, the degron construct was rapidly and fully degraded after anaphase onset as indicated by a complete drop relative degron-eGFP signal. As expected, the prey-mCherry signal was maintained after anaphase onset.

Remarkably, in the presence of rapalog, we observed three different localization patterns between degron-eGFP and prey-mRuby signals with different degradational outcomes (Figure 3C). First, we observed colocalization between the degron-eGFP signal and the prey-mRuby signal before and after anaphase onset (top panel, Figure 3C). Similar to previous results, this resulted in partial degradation of the degron construct, maintaining the degron-eGFP signal after anaphase onset. Interestingly, prey-mRuby rapidly increased over time. Secondly, we observed colocalization between the degron-eGFP signal and the prey-mRuby signal before anaphase onset, which was lost after anaphase onset (middle panel, Figure 3C). This resulted in near-complete degradation of the degron construct, as indicated by a marginal maintained degron-eGFP signal after anaphase onset. The prey-mRuby signal was increased after anaphase onset, indicating no degradation. Thirdly, we observed no colocalization between the degron-eGFP signal and the prey-mRuby signal at all. This was indicated by a uniformly distributed localization of the degron-eGFP signal across the cell (bottom panel, Figure 3C). The degron-eGFP construct was fully degraded, as indicated by a complete drop in the relative degron-eGFP signal. The prey-mRuby signal also increased after anaphase onset, indicating no degradation. The fraction of cells exhibiting different degradational outcomes was quantified. In 19.83% of cells, colocalization was maintained after anaphase onset. In 4.31% of cells, colocalization was lost after anaphase onset, and in 75.86% of cells, colocalization did not occur at all (Figure 3D).

Our data show that rapalog-induced dimerization can result in three distinct phenotypes with differential degradation patterns. These findings indicate that, while the degron construct can induce colocalization and protect the degron from degradation, it does not achieve the desired temporal control of protein degradation. Further troubleshooting is necessary to elucidate the errors in the degron system and improve its reliability and effectiveness.

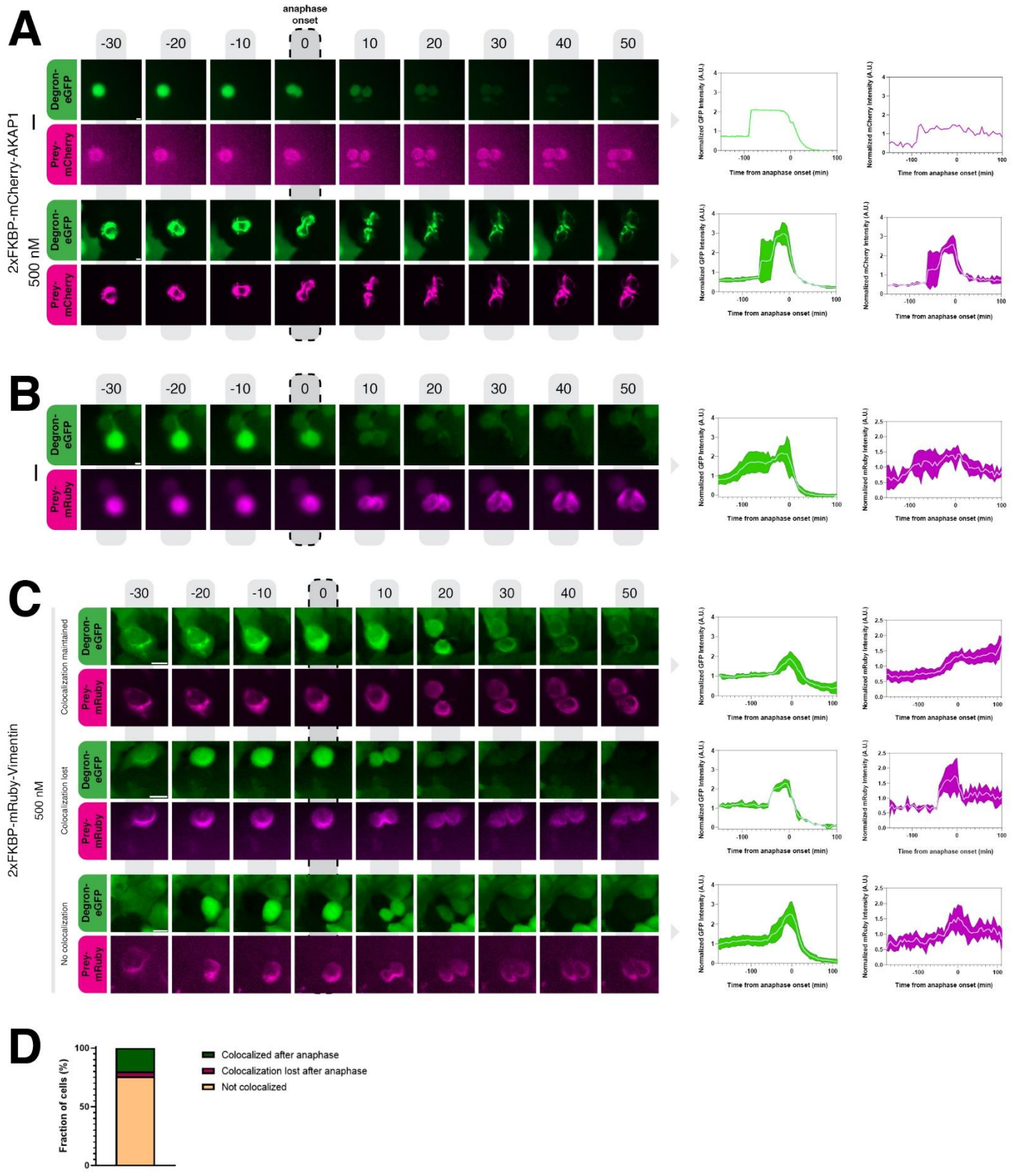

Figure 3. Rapalog-induced dimerization and its effect on degradation patterns.

(A) Live-cell imaging of U2OS$^{hGem(1:60)\text{-}eGFP\text{-}FRB}$ cells, transfected with 2xFKBP-mCherry-AKAP1. The images show degron-eGFP signal and prey-mCherry signal at various timepoints relative to anaphase onset (time 0). In the absence of rapalog, the degron is degraded after anaphase onset as indicated by decreasing eGFP expression. In the presence of rapalog, colocalization is observed and the degron is protected from degradation. Graphs on the right side indicate the quantification of degron-eGFP and prey-mRuby expression over time. The X-axis indicates the time from anaphase onset, whereas the Y-axis indicates the normalized eGFP expression as a fraction of the average intensity per timepoint (mean ± s.d. of one cell in the absence of rapalog and two cells in the presence of rapalog across one independent experiment). **(B)** Live-cell imaging of U2OS$^{hGem(1:60)\text{-}eGFP\text{-}FRB}$ cells transfected with 2xFKBP-mRuby-vimentin. In the absence of rapalog, the degron-eGFP signal and the prey-mRuby signal do not colocalize (graphs indicate mean ± s.d. of three cells across one independent experiment). **(C)** Different localization patterns resulting in differential degradational outcomes using 2xFKBP-mRuby-Vimentin as prey construct. (I) Colocalization between degron-eGFP and prey-mRuby signals before anaphase onset, resulting in a partial protection from degradation for the degron and the prey after anaphase onset. (II) Colocalization between degron-eGFP and prey-mRuby signals before anaphase onset resulting in a loss of colocalization after anaphase onset and degradation of the degron but not the prey. (III) No colocalization between the degron-eGFP signals and the prey-mRuby signals, resulting in degradation of the degron but not the prey (graphs indicate mean ± s.d. of eight cells across three independent experiments). **(D)** Quantification of fraction of cells exhibiting differential localization patterns using 2xFKBP-mRuby-Vimentin as prey construct (n=116 cells across three independent experiments).

Troubleshooting of the ineffective degron system

Despite initial observations suggesting that the degron construct degrades after anaphase onset and that the degron construct was able to recruit prey constructs, the degron system is ineffective because colocalization protects the degron from degradation. This outcome was only observed in 20% of cells, which raises questions about the overall effectiveness and reliability of the degron system. To address these questions, we undertook several troubleshooting steps, focusing on potential factors that could affect the degron system, including rapalog concentration, degron and prey concentrations, and the recruitment capability of a specific prey construct that was not linked to a protein of interest.

The first step in troubleshooting was to assess whether the rapalog concentration was sufficient to induce effective colocalization between the degron and the prey construct. We hypothesized that increasing the rapalog concentration would enhance dimerization. We increased the rapalog concentration to 4 µM, which should saturate the system, and performed live-cell imaging on U2OS$^{hGem(1:60)\text{-}eGFP\text{-}FRB}$ cells transfected with 2xFKBP-mCherry as prey construct. The results show that, in the absence of rapalog, the degron construct was rapidly degraded, as indicated by the progressive decrease in degron-eGFP signal over time. The prey-mCherry signal remains unchanged, indicating that the prey construct and the degron construct are spatially differently localized. In the presence of 4 µM rapalog, there was no significant change in the behavior of the degron and the prey. The degron construct continued to degrade after anaphase onset, and there was no observed colocalization between eGFP and mCherry fluorescence (Figure 4A). This indicates that even with a high concentration of rapalog, dimerization was not enhanced and that increasing the rapalog concentration was not sufficient to improve the effectiveness of the degron system.

Next, we considered that the relative concentrations of the degron construct and prey constructs might influence the efficiency of colocalization. We conducted several fixed-cell imaging experiments with varying ratios of degron and prey constructs. In U2OS$^{hGem(1:60)\text{-}eGFP\text{-}FRB}$ cells, we increased the expression of the degron construct by increasing the amount of doxycycline and we halved the amount of prey construct, creating a significant excess of degron construct. The results indicated that, in the absence of rapalog, the degron construct and the prey construct were spatially differently localized by showing no overlap between degron-eGFP and prey-mRuby signals. In the presence of rapalog, degron-eGFP, and prey-mRuby signals overlap significantly, indicating colocalization of the degron and the prey constructs (Figure 4B, left panel). Similar patterns are observed in HeLa cells transfected with relatively less degron construct (Figure 4B, middle panel). Interestingly, doubling the concentration of degron in HeLa cells using 2xFKBP-mCherry-Rab11 as prey construct (Figure 4B, right panel), and in the presence of rapalog, marginal colocalization between eGFP and mCherry fluorescence is observed in the nucleus, whereas distinct spatial localization is observed in the cytoplasm. Hence, adjusting the ratio of the degron and prey constructs showed some variation but did not lead to a significant improvement in the desired increase of efficient colocalization.

Overall, the results show that the degron system rarely induces dimerization between the degron and the prey constructs. When dimerized, however, this dimerization protects the degron construct from degradation. This inconsistency suggests underlying errors with the effectiveness and reliability of the degron system that could not be attributed to the rapalog concentration. Further troubleshooting is necessary to elucidate the errors in the degron system and optimize it to increase the effectiveness of colocalization. In conclusion, the degron system does not achieve the desired temporal control of protein degradation from anaphase until G1-phase.

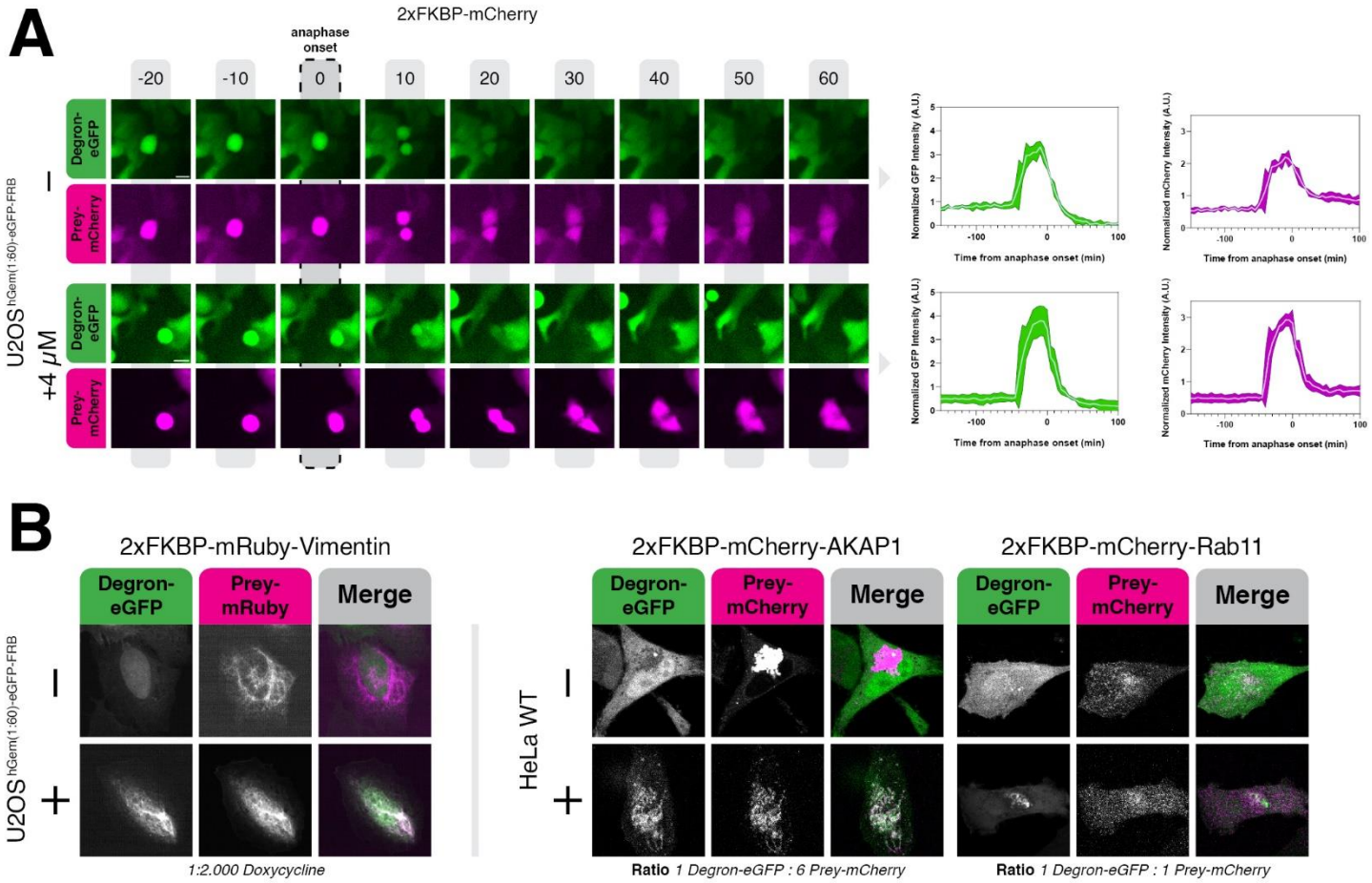

Figure 4. Troubleshooting of different components of the degron system.

(A) Live-cell imaging of U2OS$^{hGem(1:60)\text{-}eGFP\text{-}FRB}$ cells expressing hGem(1:60)-eGFP-FRB upon doxycycline induction and transfected with either 2xFKBP-mCherry. The images show eGFP fluorescence and mCherry fluorescence at various timepoints relative to anaphase onset (time 0). The corresponding graph shows the quantification of degron-eGFP signal and prey-mCherry signal overtime. The X-axis indicates the time from anaphase onset, whereas the Y-axis indicates the normalized eGFP/mCherry expression as a fraction of the average intensity per timepoint (mean ± s.d. of three representative cells across one independent experiment). **(B)** Fixed-cell imaging of U2OS$^{hGem(1:60)\text{-}eGFP\text{-}FRB}$ cells and HeLa WT cells with various concentrations of degron and prey constructs. For U2OS$^{hGem(1:60)\text{-}eGFP\text{-}FRB}$ cells (left panel), different concentrations of Doxycycline were used for induced-expression as indicated below the panels. For HeLa WT cells (middle and right panel), the used ratios between degron and prey constructs are indicated below the panels. n=3 cells per condition across one independent experiment.

Discussion

In this thesis, we investigated whether APC/C^{Cdh1} can be utilized to develop an inducible system for the temporal degradation of proteins from anaphase until G_1-phase. Our data demonstrate that the presence of rapalog induces colocalization between degron and various prey constructs (Figure 3). However, live-cell imaging revealed a low dimerization efficiency between the degron and the prey (~20%), and this dimerization resulted in the degron being partially protected from degradation.

Marginal colocalization between the degron and the prey in the presence of rapalog

A concentration of 4 µM was insufficient to induce dimerization between the degron construct and a 2xFKBP-mCherry prey construct, as demonstrated in Figure 4A. However, the experiment was carried out using a prey construct that was not linked to a protein of interest, by which a distinct localization pattern of this particular prey construct could not be observed. The experiment might be more suitable with a prey construct with a clearer localization pattern, such as filamentous vimentin or AKAP1. In our experiments, cells were supplemented with rapalog one hour before fixation or continuously incubated in the rapalog-containing culture medium during live-cell imaging. Since rapalog effects should occur within 15 minutes to 1 hour in the presence of rapalog, the incubation time should be sufficient to induce dimerization. Moreover, as the same rapalog vial was used for both fixed-cell and live-cell imaging, the effectiveness of the rapalog was confirmed. Despite this, we observed a loss of colocalization after anaphase onset, even in the presence of rapalog. This led us to hypothesize that the dimerization was not strong enough to maintain upon degradation by the 26S proteasome. To address this, we aimed to increase the strength of the dimerization by switching from an FRB-FKBP system to a SpyTag-SpyCatcher system, which forms an irreversible covalent bond between the SpyCatcher domain linked to the degron and the SpyTag domain linked to the prey. However, future experiments are required to verify or refute this hypothesis.

The degron escapes proteasomal degradation when colocalizing the prey construct

To understand how proteins can be protected from degradation by the 26S proteasome, we need to consider the criteria required for proteins to be targeted for proteasomal degradation and the ubiquitin-mediated proteasomal degradation process itself. Proteasomal degradation of geminin is a three-step process in which its destruction box (D-box or in this case hGem(23:31))[12] is first recognized by the E3-ligase APC/C^{Cdh1}, subsequently linked to ubiquitin molecules, and lastly unfolded and committed to an irreversible process of degradation by the 26S proteasome. In each step of the process, several hypotheses can be explored.

The ubiquitination cascade initiates by ubiquitin-activating enzymes (E1) binding to ubiquitin proteins and ATP, after which it is transferred to ubiquitin-conjugating enzymes (E2) that is recruited to a ubiquitin ligase (E3) that recognizes a substrate's D-box. Possibly, the D-box can be buried inside the three-dimensional conformation of the dimerized construct. However, as each component of the degron construct is separated by a flexible GS-linker, hence increasing the intrinsic flexibility, the degron can undergo conformational changes by which the D-box should not be permanently buried. Furthermore, the degron was designed to position hGem(1:60) at the C-terminus, by which the likelihood of the buried D-box hypothesis decreases.

Subsequently, we questioned whether the recognition of geminin by APC/C^{Cdh1} is so specific that a dimerization between degron and prey constructs could result in APC/C^{Cdh1} no longer

recognizing geminin as a substrate. During the S and G_2-phases, geminin binds and sequesters Cdt1 proteins to inhibit a second round of DNA replication. Interestingly, over-expression of geminin inhibits ubiquitination of Cdt1, by which it is protected from degradation. However, the exact mechanism by which geminin achieves this has not been elucidated[13,14]. In our experiment, in which we reduced the amount of degron construct (Figure 4B, left panel), we observed no significant differences in localization patterns. It would be interesting to observe in a live-cell imaging experiment whether a decrease in the amount of degron construct could result in no protection from degradation anymore. Next, we wondered whether the ubiquitination of hGem(1:60) solely is enough to mark the entire dimerized construct for degradation. Previous research indicates that, when ubiquitinated domains are associated with proteins that lack ubiquitination, the entire protein complex is still marked for degradation by acting as a ubiquitination adaptor[15]. This is supported by a study in 2016 where researchers created an FRB-FKBP degron system. In this system, a single trans-located ubiquitin-like domain (UbL) led to the degradation of the entire dimerized construct[16].

The 19S regulatory cap of the 26S proteasome utilizes ATPase complexes to unfold ubiquitinated protein substrates[17]. To allow the unfolding of proteins, ubiquitinated proteins must contain intrinsically or induced disordered regions (IDRs) to function as a degradation initiation site for the 26S proteasome[18–20]. The individual domains in the hGem(1:60)-eGFP-FRB construct are linked by flexible GS-linkers which, besides their connecting function, simultaneously function as IDRs and hence play functional roles in proteasomal degradation[21]. In an FRB-FKBP degron system, researchers created two constructs: a ubiquitin-like domain (UbL) linked to mCherry, an FRB domain, and a maltose binding protein (MBP) domain (I) and an FKBP domain linked to GFP, and a 35 amino acids-long disordered tail (II)[16]. importantly, these researchers found that this tail is crucial for proteasomal degradation, supported by the idea that the 26S proteasome requires a 20-30 amino acids-long tail to initiate proteasomal degradation[22]. When the researchers removed the tail from the target protein, they observed protection of degradation, even in the presence of rapalog. Thus, the lack of an initiation tail in our construct seems like a highly plausible explanation for escaping degradation by the 26S proteasome. However, future cloning of the proteasomal initiation tail into the construct of interest must indicate whether this hypothesis is to be verified or refuted. At last, the size of the dimerized construct must be considered. The 26S proteasome is a relatively large (2.5 mDa) protein complex that can degrade the largest known human protein, titin, with a size of approximately 3.0 mDa[23]. Therefore, the hypothesis that the dimerized construct is too large for proteasomal degradation, can be refuted.

In summary, while this thesis demonstrates that our degron system is ineffective, the utilization of APC/C^{Cdh1} for an inducible and temporal degradation system from anaphase until G_1-phase still offers high potential. To address the marginal colocalization between the degron and prey constructs in the presence of rapalog, we recommend conducting a new dose-response assay that includes various prey constructs with distinct localization patterns, such as vimentin and AKAP1 (I). Furthermore, we recommend setting the SpyTag/SpyCatcher system up to evaluate whether a covalent bond increases dimerization between degron and prey constructs (II). To understand why the degron is protected from degradation when colocalizing the prey construct, we recommend conducting live-cell imaging with a decreased amount of degron construct to limit the amount of geminin (I) and cloning an unstructured tail into prey constructs to facilitate unfolding by the 26S proteasome (II). Performing these experiments is essential to determine whether the system can be made to work effectively, after which the system can be used for its defined purpose: endogenous protein degradation after anaphase onset until G_1-phase.

Materials and Methods

Cell culture

U2OS$^{hGem(1:60)\text{-}eGFP\text{-}FRB}$ cells (a gift from Wilco Nijenhuis) and HeLa WT cells were cultured in DMEM High Glucose (4.5 g/L) (Capricorn Scientific, DMEM-HPSTA) supplemented with 10% Tet-approved FBS, and penicillin and streptomycin (ThermoFisher Scientific, 15140122). All cells were kept at 37°C and 5% CO_2.

Transfection

Cells used for fixed-cell imaging were seeded in 12-well plates (ThermoFisher Scientific, 150628) at 30-40% confluency, whereas cells used for live-cell imaging were seeded in 8-well Ibidi chambers (Ibidi GmbH, 80801). Cells were transfected the following day using Lipofectamine™ 2000 transfection reagent (ThermoFisher Scientific, 11668019). The DNA:Lipofectamine™ 2000 ratio was maintained across experiments while adjusting the ratio according to the surface area of the wells. For a surface area of 1 cm^2, 200 ng of DNA and 1.2 µl of Lipofectamine™ 2000 were incubated in 55 µL Opti-MEM™ (ThermoFisher Scientific, 11058021) for 5 minutes at room temperature. Exceptions for the DNA concentrations are marked as ratios in Figures 2A and 4B. Next, the DNA mixture was added to the transfection mixture for 20 minutes at room temperature and added dropwise to the cells. The transfection mixture was incubated at 37°C for approximately 5 hours and then replaced with fresh warm DMEM as described above. Transfected cells were incubated at 37°C for 24 hours before live-cell imaging or fixation.

For fixation, cells were fixed using 4% Paraformaldehyde in PBS for 10 minutes and rinsed three times with PBS for 5 minutes. Subsequently, fixed cells were mounted using ProLong™ Diamond Antifade Mountant (ThermoFisher Scientific, P36965).

Drug treatment

To induce dimerization, different concentrations of A/C Heterodimerizer (rapalog) (Takara, 635056) were added to cells 1 hour before fixation or live-cell imaging, as indicated in the figures. To induce expression of hGem(1:60)-eGFP-FRB, different concentrations of Doxycycline were added 24 hours before fixed-cell imaging and live-cell imaging, as indicated in the figures.

Microscopy

Fixed-cell imaging

Images from Figure 2A were acquired on a Zeiss LSM 700 microscope equipped with a 63x (Plan Apochromat) oil-immersion objective. The laserlines used were the 488 nm (GFP) and 555 nm (mCherry/mRuby). Images were acquired with a Nikon DS-Qi2 Mono Digital Microscope Camera. The microscope was controlled using Nikon NIS Br software (Tokyo, Japan).

Live-cell imaging

Images from Figures 1C, 3A-C, and 4A were acquired on a Nikon Ti microscope equipped with a 20x (Plan Apochromat) dry objective with Perfect Focus System. Cells were kept at 37°C and 5% CO_2 with a Tokai-Hit. Color filters used were the chroma ET-GFP (49002) and chroma ET-mCherry (49008). The microscope was controlled using MicroManager software (San Diego, USA). Images were acquired every 5 minutes.

Image analysis

Images were analyzed using ImageJ Fiji[24]. For intensity analysis, regions of interest (ROIs) were drawn around the cell in each frame. Of each ROI, the mean gray values were measured, of which the background intensity was subtracted. Subsequently, the mean gray value was normalized to the average intensity across 200 frames. The normalized Graphs were generated using GraphPad Prism 8 (San Diego, USA). Subsequent figures were assembled using InDesign. Cartoons used in the figures were created using BioRender.

References

1. Yang, Y., Xu, J., Ge, S. & Lai, L. CRISPR/Cas: Advances, Limitations, and Applications for Precision Cancer Research. *Front Med (Lausanne)* **8**, 649896 (2021).

2. Yu, A. M., Choi, Y. H. & Tu, M. J. RNA Drugs and RNA Targets for Small Molecules: Principles, Progress, and Challenges. *Pharmacol Rev* **72**, 862 (2020).

3. Ditchfield, C. *et al.* Aurora B couples chromosome alignment with anaphase by targeting BubR1, Mad2, and Cenp-E to kinetochores. *J Cell Biol* **161**, 267–280 (2003).

4. Sun, L. *et al.* A Septin Cytoskeleton-Targeting Small Molecule, Forchlorfenuron, Inhibits Epithelial Migration via Septin-Independent Perturbation of Cellular Signaling. *Cells* **9**, (2020).

5. Tuan, N. M. & Lee, C. H. Role of Anillin in Tumour: From a Prognostic Biomarker to a Novel Target. *Cancers (Basel)* **12**, 1–27 (2020).

6. Yesbolatova, A. *et al.* The auxin-inducible degron 2 technology provides sharp degradation control in yeast, mammalian cells, and mice. *Nature Communications 2020 11:1* **11**, 1–13 (2020).

7. Sakaue-Sawano, A. *et al.* Visualizing spatiotemporal dynamics of multicellular cell-cycle progression. *Cell* **132**, 487–498 (2008).

8. McGarry, T. J. & Kirschner, M. W. Geminin, an inhibitor of DNA replication, is degraded during mitosis. *Cell* **93**, 1043–1053 (1998).

9. Schrock, M. S., Stromberg, B. R., Scarberry, L. & Summers, M. K. APC/C ubiquitin ligase: functions and mechanisms in tumorigenesis. *Semin Cancer Biol* **67**, 80 (2020).

10. Banaszynski, L. A., Liu, C. W. & Wandless, T. J. Characterization of the FKBP.rapamycin.FRB ternary complex. *J Am Chem Soc* **127**, 4715–4721 (2005).

11. Rollins, C. T. *et al.* A ligand-reversible dimerization system for controlling protein-protein interactions. *Proc Natl Acad Sci U S A* **97**, 7096–7101 (2000).

12. Dimaki, M. *et al.* Cell Cycle-dependent Subcellular Translocation of the Human DNA Licensing Inhibitor Geminin. *J Biol Chem* **288**, 23953 (2013).

13. Ballabeni, A. *et al.* Human geminin promotes pre-RC formation and DNA replication by stabilizing CDT1 in mitosis. *EMBO J* **23**, 3122–3132 (2004).

14. Ballabeni, A., Zamponi, R., Moore, J. K., Helin, K. & Kirschner, M. W. Geminin deploys multiple mechanisms to regulate Cdt1 before cell division thus ensuring the proper execution of DNA replication. *Proc Natl Acad Sci U S A* **110**, E2848 (2013).

15. Prakash, S., Inobe, T., Hatch, A. J. & Matouschek, A. Substrate selection by the proteasome during degradation of protein complexes. *Nat Chem Biol* **5**, 29–36 (2009).

16. Wilmington, S. R. & Matouschek, A. An Inducible System for Rapid Degradation of Specific Cellular Proteins Using Proteasome Adaptors. *PLoS One* **11**, (2016).

17. Martinez-Fonts, K. *et al.* The proteasome 19S cap and its ubiquitin receptors provide a versatile recognition platform for substrates. *Nat Commun* **11**, (2020).

18. Schauber, C. *et al.* Rad23 links DNA repair to the ubiquitin/proteasome pathway. *Nature* **391**, 715–718 (1998).

19. Prakash, S., Tian, L., Ratliff, K. S., Lehotzky, R. E. & Matouschek, A. An unstructured initiation site is required for efficient proteasome-mediated degradation. *Nat Struct Mol Biol* **11**, 830–837 (2004).

20. Heessen, S., Masucci, M. G. & Dantuma, N. P. The UBA2 domain functions as an intrinsic stabilization signal that protects Rad23 from proteasomal degradation. *Mol Cell* **18**, 225–235 (2005).

21. Moses, D. *et al.* Revealing the Hidden Sensitivity of Intrinsically Disordered Proteins to their Chemical Environment. *J Phys Chem Lett* **11**, 10131 (2020).

22. Bard, J. A. M. *et al.* Structure and Function of the 26S Proteasome. *Annu Rev Biochem* **87**, 697 (2018).

23. Bard, J. A. M., Bashore, C., Dong, K. C. & Martin, A. The 26S Proteasome utilizes a kinetic gateway to prioritize substrate degradation. *Cell* **177**, 286 (2019).

24. Schindelin, J. *et al.* Fiji: an open-source platform for biological-image analysis. *Nature Methods 2012 9:7* **9**, 676–682 (2012).